ГОДИШНИК НА УНИВЕРСИТЕТА ПО АРХИТЕКТУРА, СТРОИТЕЛСТВО И ГЕОДЕЗИЯ СОФИЯ

Том Volume 59 2026 Брой Issue 2

ANNUAL OF THE UNIVERSITY OF ARCHITECTURE, CIVIL ENGINEERING AND GEODESY SOFIA

DOI: 10.71167/uaceg.2026.590208

Received: 09.11.2025
Accepted: 17.01.2026

MODELING A REDUCED-ORDER REPRESENTATION OF LOCAL BUCKLING IN SHEAR-LINK MEMBERS FOR ECCENTRICALLY BRACED STEEL FRAMES

A. Sefa Guren[1], N. Shaban[2], A. Saritas[3]

Keywords: *shear link, local buckling, finite element modeling, critical averaging region, cyclic behavior*

ABSTRACT

The study presents the development of reduced-order representations for capturing inelastic cyclic behavior and local buckling effects in shear-link members of eccentrically braced steel frames. Detailed finite element (FE) models were developed in ABAQUS using shell elements with combined isotropic-kinematic hardening for steel, and validated against experimental data, showing close agreement in strength and degradation trends. A representative link specimen was analyzed under monotonic and cyclic loading, with and without geometric nonlinearity, to isolate the role of local buckling in stiffness degradation. A critical averaging region (CAR) approach was introduced to capture critical local responses in flange and web regions. Results showed that wider CARs more effectively represented the combined influence of distributed plasticity and geometric imperfections, particularly in flanges, and that geometric nonlinearity was essential to simulate buckling initiation and post-buckling softening. Uniaxial curves from the CAR study will be used to develop constitutive models capturing material and geometric nonlinearity in flange and web regions. Integrated into fiber-based frame models, these will enable efficient simulation of local buckling within global analyses, thus improving the speed and fidelity of nonlinear dynamic analyses for eccentrically braced frames.

[1] Ahmet Sefa Guren, Eng., Department of Civil Engineering, Middle East Technical University, 1 Dumlupınar Blvd., Ankara 06800, Turkiye, e-mail: sefa.guren@metu.edu.tr

[2] Nefize Shaban, Dr. Eng., Department of Civil Engineering, Middle East Technical University, 1 Dumlupınar Blvd., Ankara 06800, Turkiye, e-mail: shaban.nefize@gmail.com

[3] Afsin Saritas, Prof. Dr. Eng., Department of Civil Engineering, Middle East Technical University, 1 Dumlupınar Blvd., Ankara 06800, Turkiye, e-mail: asaritas@metu.edu.tr

1. Introduction

Eccentrically braced frames (EBFs) are essential systems for modern seismic design of steel structures. They effectively combine the stiffness of concentrically braced frames with the ductility of moment-resisting frames [1, 2]. The system's performance relies on shear-links, which are designed to deform inelastically and dissipate seismic energy, protecting the rest of the frame [3]. The primary challenge in modelling EBFs is capturing the complex behavior of these links. Under severe cyclic loading, shear-links exhibit local buckling in their flanges and webs. This buckling leads to strength degradation, stiffness softening, and narrowed hysteretic loops [4]. Accurately simulating these degradation mechanisms is essential for reliable prediction of seismic performance.

This need for accuracy creates a significant computational problem, resulting in a trade-off between fidelity and efficiency. High-fidelity models such as detailed finite element models using shell or continuum elements (e.g., utilized in ABAQUS/ANSYS) can realistically simulate local instability and post-buckling strength loss. However, their computational cost is extremely high, making them impractical for nonlinear dynamic analysis of an entire building, especially for parametric or probabilistic studies [5]. In contrast, fiber-based beam-column elements (e.g., in OpenSees) are computationally efficient and widely used for frame-level analysis. Their formulation, however, is mostly based on uniaxial behavior and the assumption that plane section remains plane. As a result, they are mechanically incapable of capturing the local buckling that governs link degradation. This creates a clear modeling gap: existing methods are either too computationally demanding to be practical (shell or continuum models) or too simplified to be accurate (fiber models).

To bridge this gap, the present study proposes a reduced-order modeling (ROM) strategy. This approach is designed to balance mechanical accuracy with computational efficiency. The methodology begins with the development of high-fidelity shell-element models in ABAQUS. These models, which incorporate combined isotropic-kinematic hardening for cyclic plasticity, are validated against experimental data to serve as a calibrated benchmark for local behavior. Based on these detailed simulations, a Critical Averaging Region (CAR) approach is introduced. The CAR is designed to isolate and capture the essential inelastic and geometric nonlinear effects in the critical flange and web regions, but in a computationally compact form. The ultimate goal is to use the constitutive relationships extracted from these CAR simulations to develop new components for fiber-based models (e.g., in OpenSees). This will enable efficient system-level analyses that can realistically account for local buckling and cyclic degradation, providing a practical and reliable tool for the performance-based seismic assessment of EBF systems.

2. Finite element model

To establish a calibrated benchmark for capturing inelastic cyclic behavior including material and geometric nonlinearity, finite element (FE) models of shear-link specimens were developed in the general-purpose FEA program ABAQUS.

2.1. Specimen details

Two different link geometries were modeled based on the experimental specimens tested by Arce [6]. These specimens represent short and intermediate length links, as shown in Fig. 1. Both models utilize the same W10×33 base section but differ in their overall length and the spacing of the intermediate stiffeners. This study focuses on these configurations to capture the full range of behaviors from shear-dominated to shear-flexure-dominated mixed failure modes.

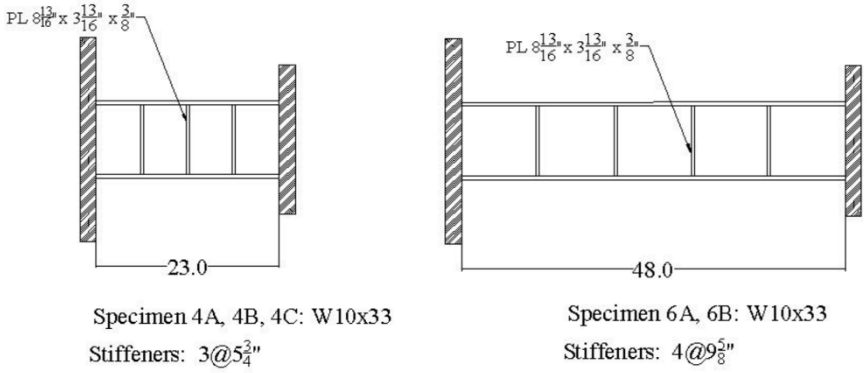

Figure 1. Shear link specimens modeled in this study, based on Arce [6] (Specimens 4 and 6 are shown, representing short and intermediate links)

2.2. Model description

All link components – including the web, flanges, and stiffeners – were modeled using 4-node shell elements with reduced integration (S4R). This element type is well-suited for accurately simulating local buckling behavior. A uniform mesh size of 10 mm was adopted after a refinement study confirmed that further reduction yielded no significant change in the results. All components are meshed uniformly.

2.3. Material properties

All components were modeled using A992 structural steel. The plastic behavior was defined using a Von-Mises yield criterion with an associated flow rule. To realistically represent the material's response under cyclic loading, a combined isotropic-kinematic hardening model was implemented. The hardening parameters are adopted from [7]:

- Isotropic Hardening: $Q_\infty = 50$ MPa and $b = 1, 2$;
- Kinematic Hardening: $C_1 = 7993$ MPa, $\gamma_1 = 175$, $C_2 = 7100$ MPa, $\gamma_2 = 116$, $C_3 = 2650$ MPa, $\gamma_3 = 60$.

The welds were not modeled explicitly since no weld failure happened in the experiment to influence link response. The properties of the materials such as yield stress and ultimate stress are assumed to be same as measured values in the Arce [6] experiment. Based on reported tensile test results, the flange and web materials of the W10×33 section exhibited yield strengths of 356 MPa and 382 MPa, ultimate strengths of 507 MPa and 503 MPa, and elongations of 33 % and 34 %, respectively.

2.4. Boundary conditions

The boundary conditions, depicted in Fig. 2, were adapted from the test setup model used by [8].

- At the left end of the link, all nodes were constrained to translate equally in the horizontal direction.
- At the right end, nodes were constrained against all DOFs except vertical translation. The cyclic load was applied to these nodes as a prescribed vertical displacement.

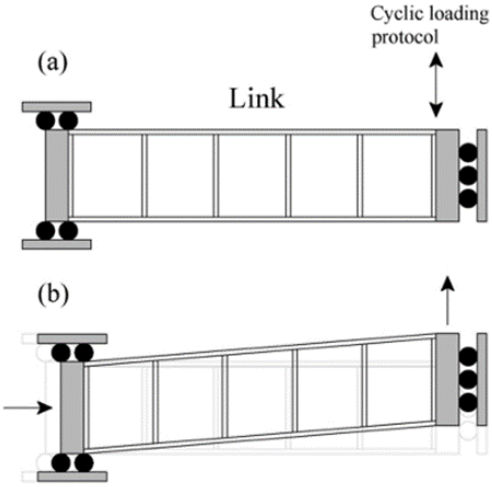

Figure 2. Schematic representation of boundary conditions

The analysis included both material and geometric nonlinearities to capture large deformations and post-buckling behavior. The models relied on their natural asymmetry developed as the web and flange elements began to yield during the early stages of loading to trigger inelastic local buckling at higher link rotation levels.

3. Validation against experimental data

The fidelity of the finite element models was validated against the experimental results for A992 steel links tested by Arce [6]. The two specimens modeled (4B and 6B) used dimensions and a cyclic loading protocol identical to the experiments.

The models accurately captured the distinct failure modes of the different link types. Figure 3 shows the short link (4B), which exhibits a shear-dominated failure. Figure 4 shows the intermediate link (6B), which experiences significant local buckling in the flanges and web near the supports. Figure 5 provides a detailed view of this localized buckling. In all cases, the deformed shape and buckling patterns of the numerical models show strong qualitative agreement with the experimental photographs.

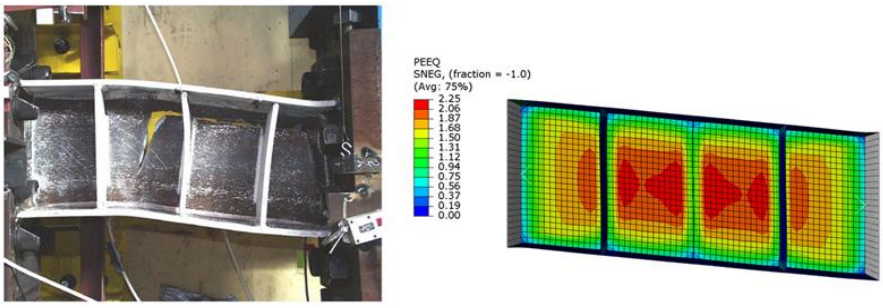

Figure 3. Deformed geometry of the short link (4B) in the experiment & numerical model

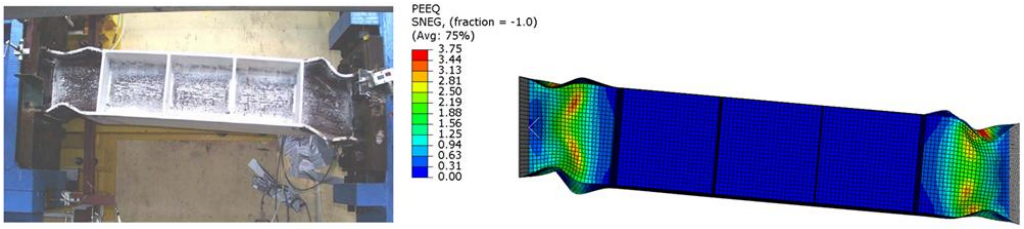

Figure 4. Deformed geometry of the intermediate link (6B) in the experiment & numerical model

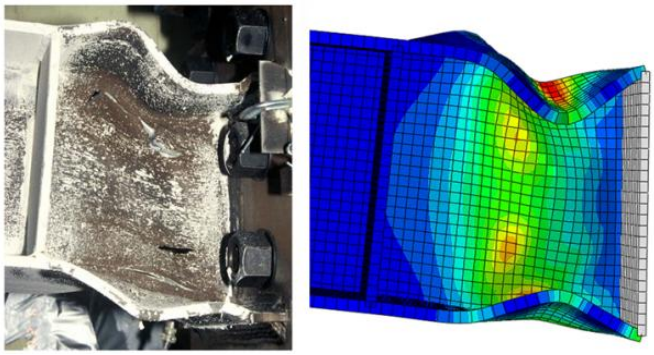

Figure 5. Buckled region at the end of the link in the experiment and in the numerical analysis

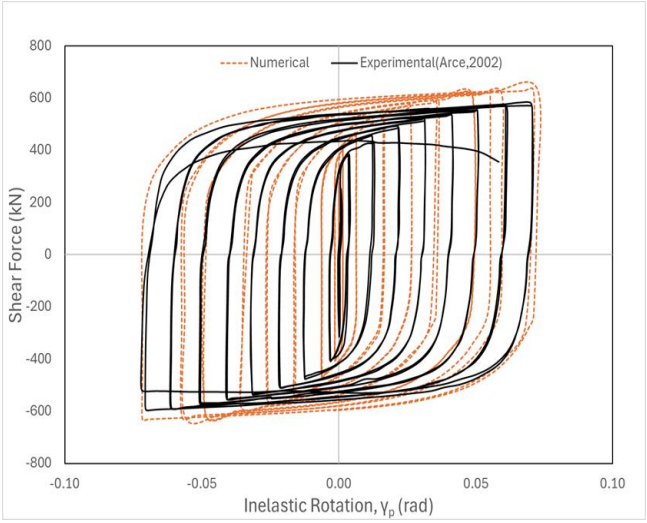

Figure 6. Numerical vs. experimental hysteretic response for 4B link

To validate the accuracy of the numerical model, the hysteretic responses were compared with the experimental findings of Arce [6]. Figure 6 shows the shear force vs. inelastic rotation for the short link (4B). Figure 7 shows the same comparison for the intermediate link (6B). The numerical model demonstrates good agreement with the experimental data, particularly in capturing the overall strength and degradation trends. However, it should be noted that the finite element models tend to be both stiffer and exhibit a slightly higher load-bearing capacity than

the experimental specimens. This discrepancy is attributed to the use of idealized boundary conditions, the absence of explicitly modeled initial geometric imperfections at the plate level, residual stresses, and local material inhomogeneities, as well as the simplified representation of connection flexibility in the shell finite element models. In addition, no macro-level geometric imperfections, such as global member out-of-straightness or initial misalignment, were considered in the numerical analyses.

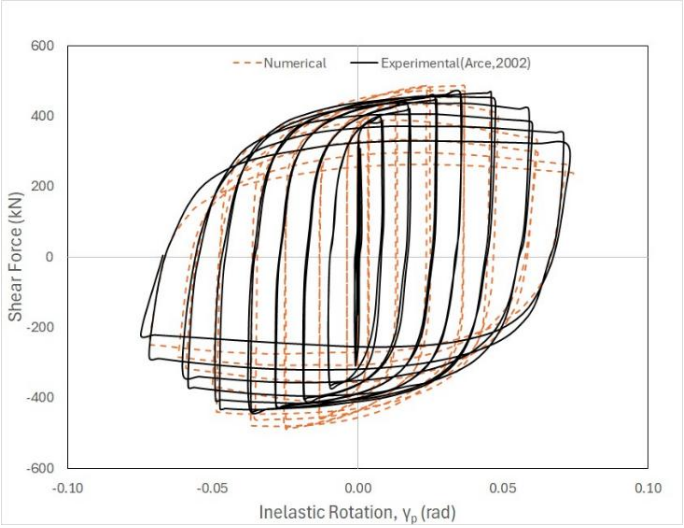

Figure 7. Numerical vs. experimental hysteretic response for 6B link

This level of agreement confirms that the high-fidelity model is a reliable benchmark for the subsequent analyses of local buckling behavior.

4. Analysis of local buckling behavior

With the FE model validated, it was used to investigate the mechanisms of local buckling and the role of geometric nonlinearity. The intermediate link (6B) was the primary focus in this regard, as its behavior is governed by the complex interaction of plasticity and geometric instability.

4.1. Stress distribution and localization

Under cyclic loading, the model shows significant stress localization near the link ends, specifically in the flange and web panels between the end supports and the first stiffeners. Figure 8 displays the normal (S22) and shear (S12) stress contours in these critical regions. The deformed shape confirms that both plasticity and buckling are concentrated near the supports, while the midspan of the link remains largely elastic.

Internal free-body cuts of the flange and web (Fig. 9) further illustrate this localization, showing how stresses redistribute as the local buckling happens. This observed localization is precisely what simpler fiber models cannot capture and is the primary driver of link degradation.

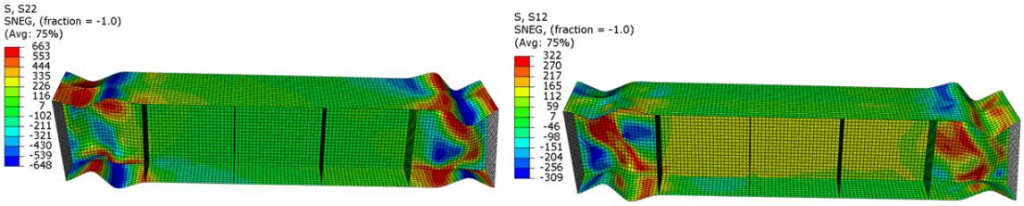

Figure 8. Normal and shear stress distribution in 6B link under cyclic loading

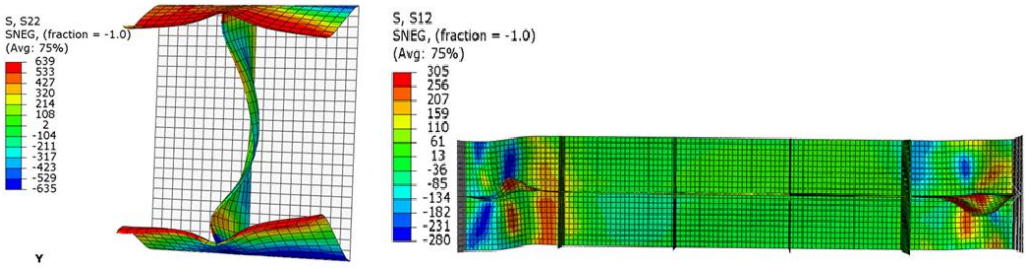

Figure 9. Free-body cut of the flange showing localized plasticity and the web showing stress redistribution

4.2. The role of geometric nonlinearity

To isolate the specific cause of buckling, two sets of analyses were performed: one with geometric nonlinearity enabled and one with it disabled.

This comparison was first conducted at the element level using monotonic loading. Figure 10 (Geometric Nonlinearity OFF) shows the normal stress in a single flange element. The material simply hardens as it is compressed. Figure 11 (Geometric Nonlinearity ON) shows the same element. Once a critical compressive stress is reached, the element locally buckles, leading to a sudden drop in stiffness and a subsequent softening response.

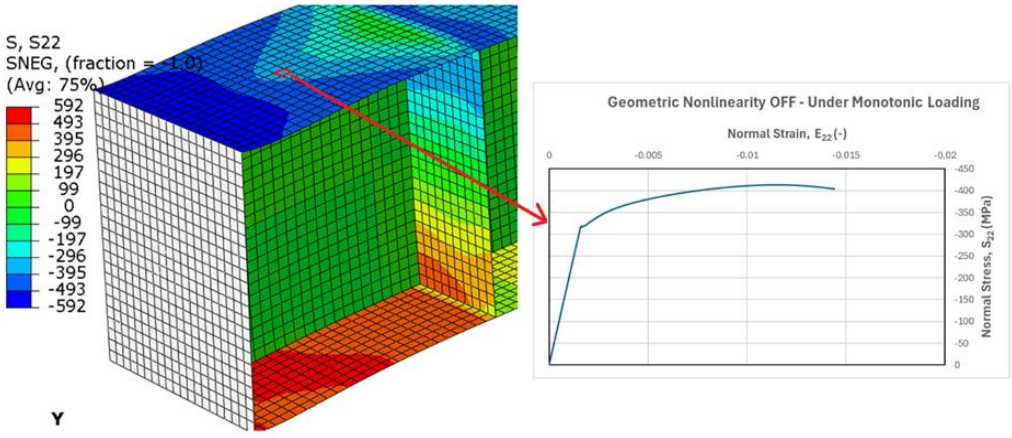

Figure 10. Normal stress in a selected element under monotonic loading (linear geometry)

This same effect is then observed at the global link level. Figure 12 (cyclic) and Figure 13 (monotonic) compare the total link shear force vs. displacement for the Geometric Nonlinearity ON and Geometric Nonlinearity OFF models. The Geometric Nonlinearity OFF model (linear geometry) overestimates the link's strength and shows no degradation. The Geometric Nonlinearity ON model (nonlinear geometry) correctly captures the post-buckling softening and strength degradation as displacement increases. These results confirm that geometric nonlinearity is the critical mechanism responsible for initiating local buckling and the associated stiffness and strength degradation. Any reduced-order model must be able to replicate this phenomenon.

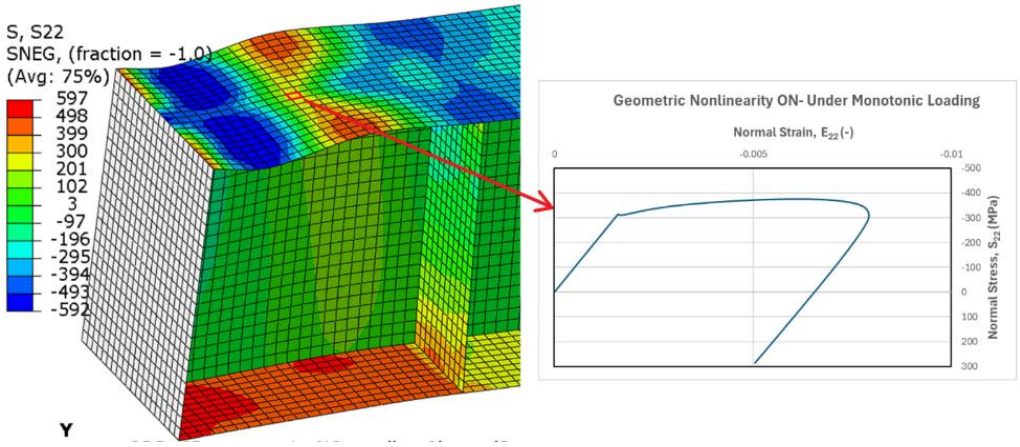

Figure 11. Same element under nonlinear geometry – local buckling observed

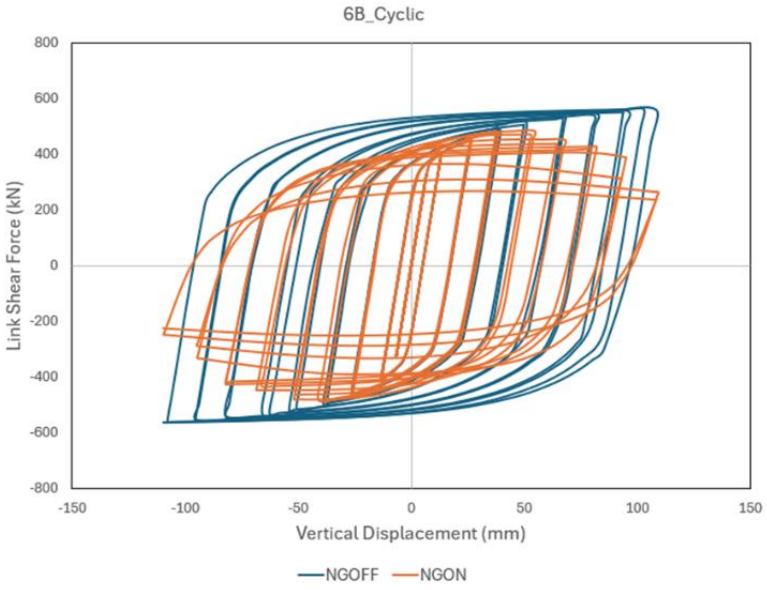

Figure 12. Link shear force comparison (cyclic) – nonlinear geometry ON vs. OFF

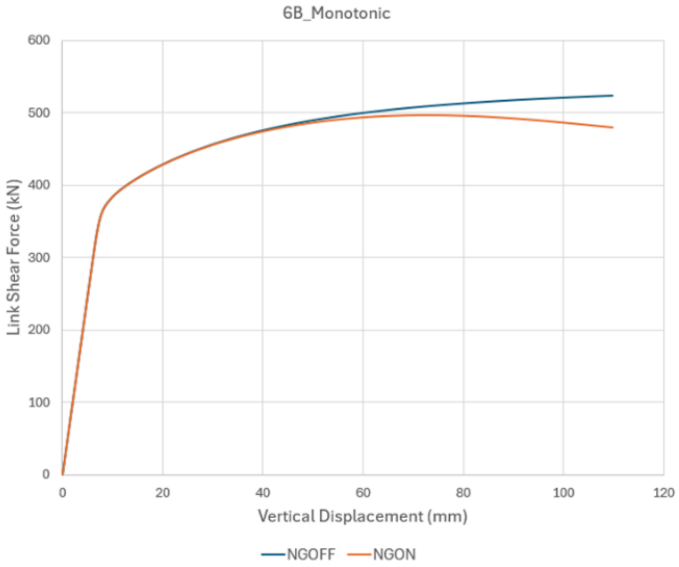

Figure 13. Link shear force comparison (monotonic) – nonlinear geometry ON vs. OFF

5. Critical Averaging Region (CAR) strategy

The previous sections established that local buckling is a critical, complex phenomenon and that high-fidelity models, while accurate, are computationally expensive. This section proposes a Critical Averaging Region (CAR) strategy to capture the essential local behaviors in a computationally efficient manner.

5.1. CAR methodology

The objective of the CAR approach is to isolate the critical regions of the link (flange and web panels near the supports) and extract their spatially averaged, uniaxial stress-strain response. This response, which inherently contains the complex information of material hardening and geometric instability, can then be used to create a simplified, fast-running model.

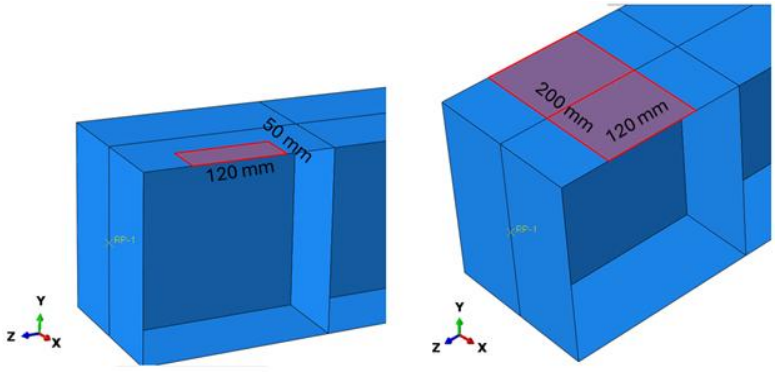

Figure 14. CAR strategies for the flange

To examine the influence of the considered region size, two strategies were implemented:

- Approach 1: A small region centered at the location of maximum stress/buckling (e.g., mid-flange or web panel).
- Approach 2: A wider strip extending across the full width of the flange or web.

These two CAR strategies are depicted in Fig. 14 (for the flange) and Fig. 15 (for the web).

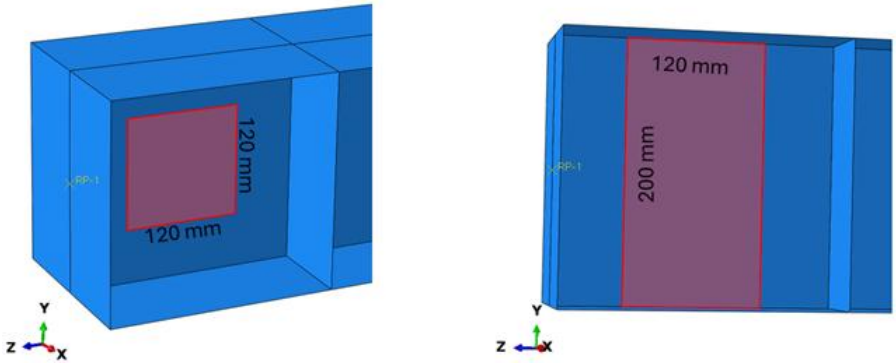

Figure 15. CAR strategies for the web

The stress and strain responses for these regions were then spatially averaged. The averaged stress $\bar{\sigma}(t)$ is calculated using the relation:

$$\bar{\sigma}(t) = \frac{\sum_{i=1}^{n_e} \sigma^{(i)}(t) \cdot S^{(i)}}{\sum_{i=1}^{n_e} S^{(i)}}, \tag{1}$$

where $\sigma^{(i)}(t)$ is the stress in element i at time t;

$S^{(i)}$ – the spatial domain (e.g., volume or area) of element i.

In the context of the shell finite element formulation, the stress $\sigma^{(i)}(t)$ refers to the section-averaged membrane stress component associated with element i. For flange regions, the longitudinal membrane normal stress is considered dominant and is therefore used in the averaging procedure. For web regions, the membrane shear stress component governs the response and is adopted as the primary measure, while acknowledging that normal stresses may also contribute to local buckling behavior in longer links. The membrane stresses employed in the averaging process are obtained from the shell formulation as through-thickness integrated quantities and thus inherently reflect the nonlinear stress redistribution through the shell thickness associated with buckling.

For a uniform shell mesh and constant thickness, this simplifies to an arithmetic mean of the stress in all n_e elements within the CAR. The same method was used to evaluate the average strain.

5.2. CAR results and comparison

The stress-strain behavior of the CAR regions was analyzed under both cyclic and monotonic conditions.

5.2.1. Flange behavior

For the flange, the choice of CAR size has a significant impact. Fig. 16 shows the behavior of CAR regions under cyclic loading. The wider stripe (Approach 2) accumulates higher compressive stress and strain. This suggests it more accurately represents the combined influence of distributed plasticity and geometric imperfections across the panel. Figure 17 shows it under monotonic loading and same trend holds. The wider stripe (Approach 2) shows a milder post-buckling softening response, while the smaller CAR (Approach 1) shows a more abrupt drop in strength.

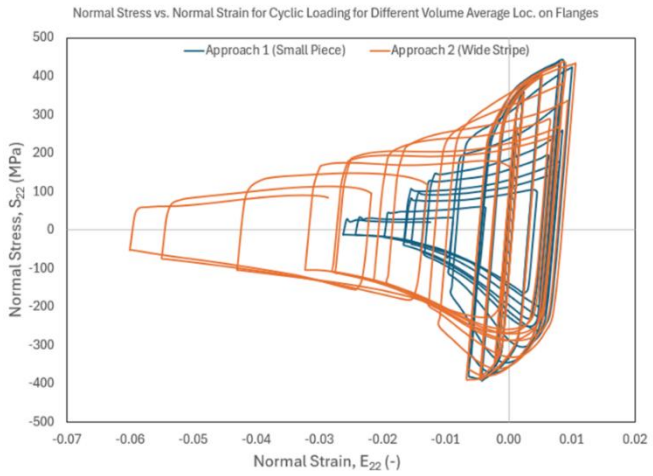

Figure 16. Comparison of normal stress in flange CARs under cyclic loading

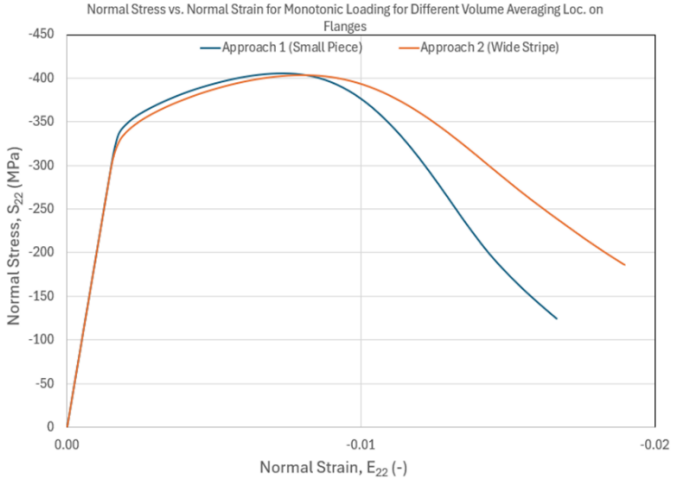

Figure 17. Comparison of normal stress-strain in flange CARs under monotonic loading

5.2.2. Web behavior

For the web, the primary behavior is shear. The cyclic shear stress-strain analysis shows significant degradation over cycles due to local web buckling in Fig. 18. Both CAR approaches capture this, although the wider region (Approach 2) initially predicts lower stress because it

includes low-stress regions near the stiffeners. Under monotonic shear, buckling does not occur, and stresses increase smoothly. As a result, both CAR approaches yield nearly identical results, which can be seen in Fig. 19.

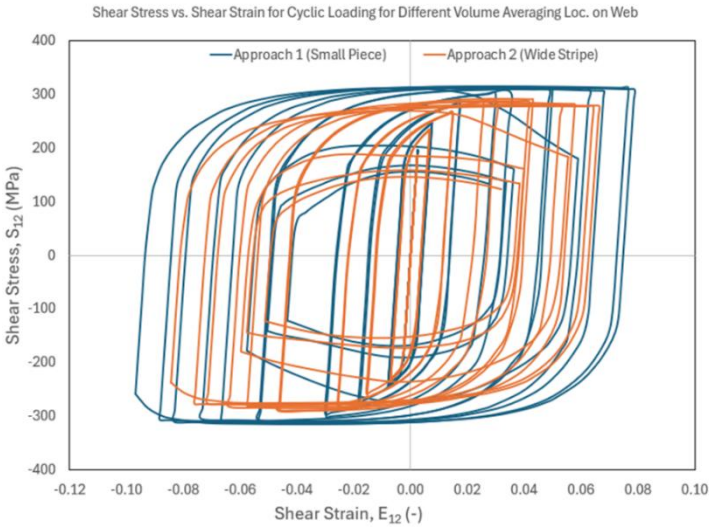

Figure 18. Shear stress-strain in web CARs under cyclic loading

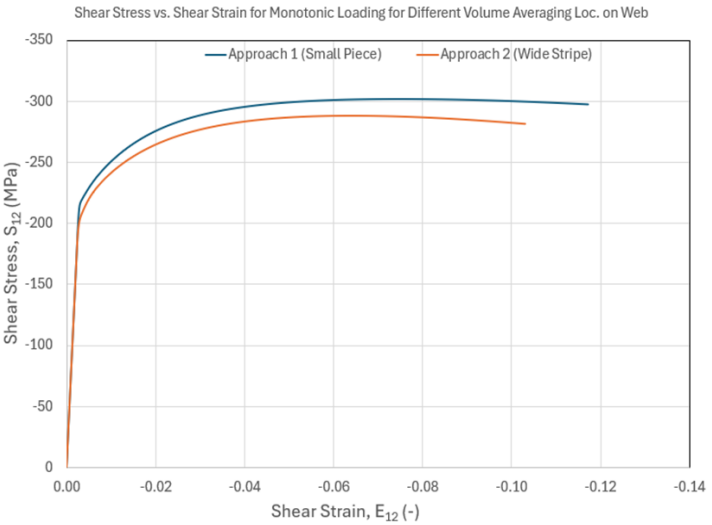

Figure 19. Shear stress-strain in web CARs under monotonic loading

5.3. Discussion

The comparisons in Fig. 16 and Fig. 17 (which overlay cyclic and monotonic responses for each CAR) highlight the key finding: the wider CAR (Approach 2) is more effective at capturing the distributed effects of buckling and plasticity, especially in the flange regions. The "small piece" (Approach 1) is overly sensitive to the behavior of a few elements, whereas the

"wide stripe" (Approach 2) provides a more stable and representative average of the panel's behavior. This approach is also consistent with similar CAR strategies in the literature [9] conducted for steel columns. Therefore, the constitutive relationships derived from the Wide Stripe (Approach 2) CARs are selected as the most suitable candidates for developing the final reduced-order model.

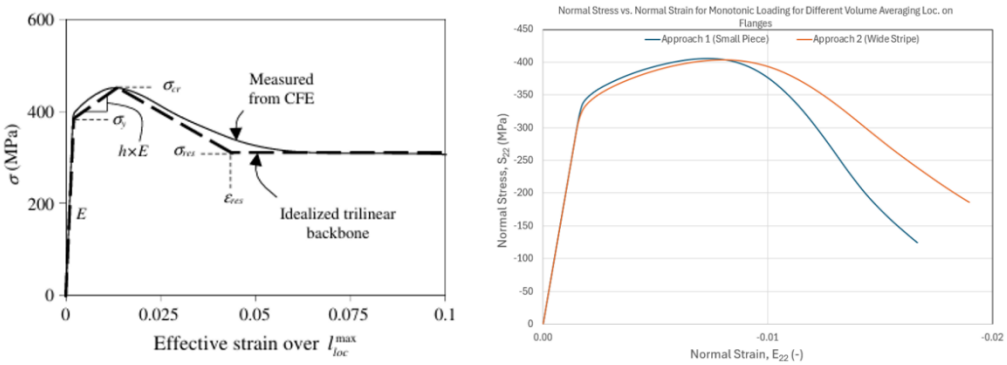

Figure 20. CAR comparison with Kolwankar et al. [9]'s approach

6. Conclusions

This study developed and utilized high-fidelity finite element models to investigate local buckling in shear-links and to establish a methodology for a reduced-order model.

6.1. Summary of findings

The key findings of this study center on the development of a robust high-fidelity finite element model and its use in creating a reduced-order modeling strategy. First, a high-fidelity model was developed in ABAQUS using S4R shell elements and a combined isotropic-kinematic hardening law. This model demonstrated its accuracy by showing good agreement with the experimental results of Arce (2002), successfully capturing the hysteretic behavior and distinct failure modes of short and intermediate links. This validated model was then used to confirm that geometric nonlinearity is the essential mechanism driving local buckling; models with this feature disabled failed to capture any strength degradation, while the full model accurately simulated the post-buckling softening. Furthermore, the analysis demonstrated that plasticity and buckling are highly localized in the flange and web panels near the link ends. This localization explains why standard fiber-based elements, which assume plane sections remain plane, are unable to capture this behavior. To address this gap, a Critical Averaging Region (CAR) strategy was proposed to develop the unique uniaxial stress-strain relations for the local buckling regions of steel shear-links. A comparison of two strategies revealed that a "Wide Stripe" (Approach 2), which averages the response over the full panel width, is superior to a "Small Piece" (Approach 1), as it provides a stable and representative stress-strain curve that effectively captures the combined, distributed effects of geometric instability and plasticity.

6.2. Future work and impact

The results of this study serve as the direct foundation for developing a computationally efficient model for system-level analysis with nonlinear frame finite element models.

The central challenge in simplified structural modeling is that local buckling induces softening, i.e. strength degradation, which causes conventional fiber-based models to suffer from "pathological mesh dependence". As Kolwankar [9] demonstrated for steel columns, this occurs because the model lacks a physical length scale, causing strain to localize to a single element. Kolwankar [9] solved this by developing a nonlocal formulation that averages strains over a characteristic length derived from continuum finite element (CFE) analysis.

Our CAR approach achieves a similar goal for steel shear-links. The stress-strain curves obtained from the "Wide Stripe" CAR (Approach 2) result from spatial averaging over a finite structural region, thereby capturing the combined effects of material nonlinearity and geometric instability in a consistent and mesh-insensitive manner.

The clear next step, which is the primary goal of our ongoing research, is to use these calibrated uniaxial curves to develop and implement new constitutive models (e.g., specialized nonlinear springs or fiber definitions). These new components will be integrated into the OpenSees framework, enabling, for the first time, a distributed plasticity frame element that can accurately and efficiently account for local buckling in steel shear-links. This will bridge the gap between high-fidelity shell models and fiber models, providing a practical tool for reliable nonlinear analysis of eccentrically braced steel frame systems.

Acknowledgements

The research study is supported by the Scientific and Technological Research Council of Türkiye (TUBITAK) under Project no: 222M144.

REFERENCES

1. *Volynkin, D*. Development and validation of shear links for LCF and EBF seismic systems via testing and numerical modelling, Ph.D. thesis, The University of Auckland, 2016.

2. *Clifton, C., Bruneau, M., MacRae, G., Leon, R., Fussell, A.* Steel building damage from the Christchurch earthquake series of 2010/2011. // Journal of the Structural Engineering Society New Zealand Inc., vol. 24, no. 2, 2011.

3. *Popov, E. P., Engelhardt, M. D.* Cyclic behavior of steel beams and connections. Journal of Structural Engineering, vol. 114, no. 8, pp. 1608 – 1629, 1988.

4. *Kasai, K., Popov, E. P*. General behavior of WF steel shear link beams. // Journal of Structural Engineering, vol. 112, no. 2, pp. 362 – 382, 1986, doi: 10.1061/(ASCE)0733-9445(1986)112:2(362).

5. *Kızıldağ, Y.* Finite element modeling approaches and comparative study on the nonlinear behavior of steel shear-links. M.S. thesis, Dept. of Civil Eng., Middle East Tech. Univ., Ankara, Turkey, 2013.

6. *Arce, G*. Impact of higher strength steels on local buckling and overstrength of links in eccentrically braced frames, Ph.D. dissertation, University of Texas at Austin, 2002.

7. *Mansouri, A.* 2021. Development of a novel haunched link for eccentrically braced frames". Eng. Struct., 245, https://doi.org/10.1016/j.engstruct.2021.112870.

8. *Richards, P. W., Uang, C. M*. Effect of flange width-thickness ratio on eccentrically braced frames link cyclic rotation capacity. J Struct Eng 2005;131(10): 1546 – 52, https://doi.org/10.1061/(ASCE)0733-9445(2005)131:10(1546).

9. *Kolwankar, S., Kanvinde, A., Kenawy, M., Lignos, D., Kunnath, ve S*. 2018. Simulating Local Buckling-Induced Softening in Steel Members Using an Equivalent Nonlocal Material Model in Displacement-Based Fiber Elements. J. Struct. Eng., 144 (10). https://doi.org/10.1061/(asce)st.1943-541x.0002189.